Physics Letters B 744 (2015) 369–374

Contents lists available at ScienceDirect

Physics Letters B

www.elsevier.com/locate/physletb

Direct determination of ground-state transition widths of low-lying dipole states in ^{140}Ce with the self-absorption technique

C. Romig [a,*], D. Savran [b,c], J. Beller [a], J. Birkhan [a], A. Endres [d], M. Fritzsche [a,1], J. Glorius [d,e], J. Isaak [b,c], N. Pietralla [a], M. Scheck [a,f,g], L. Schnorrenberger [a], K. Sonnabend [d], M. Zweidinger [a]

[a] Institut für Kernphysik, Technische Universität Darmstadt, D-64289 Darmstadt, Germany
[b] ExtreMe Matter Institute EMMI and Research Division, GSI Helmholtzzentrum für Schwerionenforschung GmbH, D-64291 Darmstadt, Germany
[c] Frankfurt Institute for Advanced Studies FIAS, D-60438 Frankfurt am Main, Germany
[d] Institut für Angewandte Physik, Goethe Universität Frankfurt am Main, D-60438 Frankfurt am Main, Germany
[e] GSI Helmholtzzentrum für Schwerionenforschung GmbH, D-64291 Darmstadt, Germany
[f] School of Engineering, University of the West of Scotland, Paisley PA1 2BE, United Kingdom
[g] SUPA, Scottish Universities Physics Alliance, Glasgow G12 8QQ, United Kingdom

ARTICLE INFO

Article history:
Received 18 August 2014
Received in revised form 23 January 2015
Accepted 8 April 2015
Available online 13 April 2015
Editor: D.F. Geesaman

Keywords:
Self absorption
Nuclear resonance fluorescence
Gamma spectroscopy
Ground-state transition width
Pygmy dipole resonance

ABSTRACT

The technique of self absorption has been applied for the first time to study the decay pattern of low-lying dipole states of ^{140}Ce. In particular, ground-state transition widths Γ_0 and branching ratios Γ_0/Γ to the ground state have been investigated in the energy domain of the pygmy dipole resonance. Relative self-absorption measurements allow for a model-independent determination of Γ_0. Without the need to perform a full spectroscopy of all decay channels, also the branching ratio to the ground state can be determined. The experiment on ^{140}Ce was conducted at the bremsstrahlung facility of the superconducting Darmstadt electron linear accelerator S-DALINAC. In total, the self-absorption and, thus, Γ_0 were determined for 104 excited states of ^{140}Ce. The obtained results are presented and discussed with respect to simulations of γ cascades using the DICEBOX code.

1. Introduction

Atomic nuclei represent enormously complex quantum objects. Their quantum states can correspond to collective modes, to non-collective single-particle excitations or to mixtures of both. This leads to complex decay patterns, in particular for collective modes situated at excitation energies where multiple lower-lying levels open alternative decay channels. However, those channels do not yet fully dominate the entire decay pattern. An important example for such a collective mode is the Pygmy Dipole Resonance (PDR) [1]. It is a resonance-like concentrated enhancement of $E1$-excitation strength in the vicinity of the particle-separation threshold. Typically, the PDR is attributed to the out-of-phase oscillation of excess neutrons against an isospin-saturated core. Recently, the PDR attracted a great deal of attention because of its fundamental character, its impact on nuclear astrophysics [2–4], and its sensitivity to properties of nuclear matter [5,6]. However, up to now the detailed structure of the PDR is not well settled (see, *e.g.*, Refs. [1,7–9] and the references therein).

Up to now, the PDR has mainly been investigated exploiting the method of Nuclear Resonance Fluorescence (NRF) (see, *e.g.*, Refs. [9–12]). NRF uses real photons to probe nuclear structure [13,14]. Owed to the low-momentum transfer of photons, they induce mainly dipole and, to a lesser extent, electric quadrupole transitions. Thus, NRF measurements are perfectly suited to study low-lying dipole states in nuclei such as states in the PDR region.

However, NRF measurements are sensitive to the product $\Gamma_0 \cdot \Gamma_0/\Gamma$ of the ground-state transition width Γ_0 and the branching ratio Γ_0/Γ to the ground state. Even though the individual transition widths Γ_i to low-lying excited states are much weaker than the branch to the ground state (*i.e.*, $\Gamma_0 \gg \Gamma_i$) this might not be the case for their sum $\sum \Gamma_i$ which is relevant for the size of Γ_0/Γ. The latter needs to be known in order to experimentally determine Γ_0 from NRF data. If, for a given state, decays to lower-lying excited states have not been observed, appropriate assumptions, *e.g.*,

* Corresponding author.
E-mail address: romig@ikp.tu-darmstadt.de (C. Romig).
[1] Present address: Canberra GmbH, D-65428 Rüsselsheim, Germany.

http://dx.doi.org/10.1016/j.physletb.2015.04.013

$\Gamma_0/\Gamma = 1$, are commonly applied. Otherwise, calculations within the statistical model can be used to estimate mean branching ratios to the ground state which has been done in NRF experiments to extract averaged properties from the spectra in an alternative analysis method (see, *e.g.*, Refs. [9,15,16]). However, a statistical approach does not help in the analysis of isolated individual states. In addition, this method has to rely on the validity of the statistical model in the investigated energy region including a reasonable description of the nucleus using level density and photon-strength functions, *i.e.*, the results are model dependent.

Recently, NRF measurements with quasi-monoenergetic photons at the High Intensity γ-Ray Source (HIγS) [17,18] at Triangle Universities National Laboratory (TUNL) in Durham, NC, USA gave experimental insight in mean decay properties of dipole excited states in the energy region of the PDR [12,19–23]. All of these measurements demonstrate that the decay via intermediate states cannot be neglected, however, the data do not answer the question how individual states behave. Recent studies also revealed that the mean branching ratio $\langle b_0 \rangle$ to the ground state cannot completely be described within the statistical model [20,22,23], demonstrating the need to study Γ_0 directly.

One opportunity to study Γ_0 is provided by inelastic proton scattering at forward angles. $B(E1)$ strengths have been extracted for individual states of ^{208}Pb below the separation threshold from (p, p') measurements [24]. However, the extraction of reduced transition strength values is model dependent. Furthermore, the energy resolution of (p, p') experiments of about 25 keV is worse than in NRF, where the resolution accounts to a few keV. Thus, the investigation of individual states in energy regions with rather high level density is difficult, especially since states with $J \neq 1$ can also strongly be excited by this mechanism.

In contrast, the method of self absorption [13,25] provides a model-independent measurement of absolute values for the ground-state transition width Γ_0, the total transition width Γ, and, therefore, also of the branching ratio to the ground state for individual states. Since self-absorption measurements are basically a combination of two NRF measurements, the excellent energy resolution of γ-ray detectors can be exploited at the same time.

In this work, we report on the first investigation of ground-state transition widths of low-lying dipole states in the PDR region in ^{140}Ce with the self-absorption technique. In the following the method of self absorption, the experimental setup and the analysis procedure is presented. Afterwards, the results are discussed and compared to simulations exploiting the DICEBOX code [26].

2. Experimental method

Commonly, in 'standard' NRF measurements the target of interest (*scatterer*) is irradiated with a photon beam, *e.g.*, bremsstrahlung, and the *decay* of states excited resonantly from the ground state is investigated. Thus, NRF is sensitive to the product of Γ_0 (excitation) and Γ_0/Γ (decay). In contrast, in self-absorption measurements absorption spectra are analyzed (see, *e.g.*, [13,25]). Hence, the *excitation* process is investigated with this method providing direct sensitivity to Γ_0. Absorption spectra are obtained when a photon beam is transmitted through a thick *absorber*. The resulting spectrum exhibits characteristic absorption lines at the resonance energies of the absorption target: photons with these energies are resonantly absorbed and, thus, missing in the absorption spectrum. The absorption lines are more pronounced for excited states with large Γ_0 so that they are a direct measure for the ground-state transition width. In addition, the transmitted spectrum has a reduced intensity with respect to the original one due to atomic attenuation effects.

Owed to the width of mostly a few eV, the absorption lines cannot be measured directly using high resolution γ-ray spectroscopy. A self-absorption experiment is, thus, usually composed out of at least two measurements. In the first one, a scattering target made of the same material as the absorber is irradiated by the absorption spectrum. With the absorber being removed from the beam line, the second measurement serves as reference measurement. The self absorption is defined as the decrease of scattered photons N_{abs} in the scattering target with respect to the number N_{nrf} of scattered photons in the measurement without absorber:

$$R = 1 - \frac{N_{abs}}{N_{nrf}}. \tag{1}$$

The decrease of scattered photons can be ascribed to resonant absorption and atomic attenuation in the absorber. By correcting R for the atomic attenuation effects, it becomes directly related to Γ_0 and the scatterer serves as high-resolution detector for resonant absorption effects. In earlier self-absorption experiments the atomic attenuation was usually accounted for by using different absorber targets: a resonant absorber (made of the material of interest) and an atomic absorber of similar Z [25,27,28]. The latter was used to measure the contribution of atomic attenuation. In the present work, we used a new approach: both measurements are performed relative to a normalization target which is included to the scattering target and ideally has only few but rather strongly excited states, in our case ^{11}B. The decrease of NRF reactions in ^{11}B is only due to atomic attenuation in the absorber. With the normalization factor $f = N_{abs}^{norm}/N_{nrf}^{norm}$ (with N_{abs}^{norm} and N_{nrf}^{norm} being the number of reactions in ^{11}B in the measurements with and without absorber, respectively) the self absorption can be corrected for the effect of atomic attenuation:

$$R_{\mathrm{exp}} = 1 - \frac{N_{abs}}{f \times N_{nrf}}. \tag{2}$$

At the same time, f also corrects for different measuring times, beam currents, dead times, and any other global normalization factor. Therefore, systematic uncertainties are strongly reduced compared to previous approaches.

For the analysis, the self absorption R has to be calculated as a function of Γ_0 and Γ. The cross section for resonant absorption of a photon corresponding to the excitation of a state j with resonance energy E_j from the ground state and the subsequent decay to a state k is described by a Breit–Wigner cross section convoluted with an energy distribution $w(E')$:

$$\sigma(E) = \int_{-\infty}^{\infty} dE' \, \frac{2\pi \left(\hbar c/E_j\right)^2 g \Gamma_0 \Gamma}{\Gamma^2/4 + (E' - E_j)^2} \times w(E'), \tag{3}$$

with $g = \frac{2J_j+1}{2J_0+1}$ being a spin-dependent statistical factor. The distribution

$$w(E')dE' = \frac{1}{\Delta\sqrt{\pi}} \cdot e^{\left(\frac{E'-E}{\Delta}\right)^2} dE', \tag{4}$$

with Δ being the so-called Doppler width, describes the distribution of effective energies E' in the rest frame of the nucleus of a photon with energy E in the laboratory system. Hence, it accounts for the finite velocities of the target nuclei within the target material and the corresponding Doppler broadening of the excitation cross section. It is used to define the resonance-absorption density

$$\alpha(z, E) = \sigma(E) \times e^{-\sigma(E)z} \tag{5}$$

with z being the penetration depth into the target. It describes the probability for resonant absorption of a photon by an excited state. The exponential term accounts for the decrease of the photon-flux

intensity at and near the resonance energy with the target due to resonant absorption. The number of photons scattered in a target can be determined by integrating the absorption density:

$$N_{\text{scatter}} = \int_{-\infty}^{\infty} dE \int_{0}^{d} dz\, \alpha(z, E), \tag{6}$$

where d is the target thickness. Eventually, using the last expression, the self absorption is calculated as

$$R_{\Gamma_0,\Gamma} = 1 - \frac{\int_{-\infty}^{\infty} dE \int_{d_A}^{d_A+d_S} dz\, \alpha(z, E)}{\int_{-\infty}^{\infty} dE \int_{0}^{d_S} dz\, \alpha(z, E)}. \tag{7}$$

Here, d_S and d_A denote the thicknesses of the scatterer and of the absorber, respectively.

3. Experiment

The self-absorption experiment on ^{140}Ce was performed at the Darmstadt High Intensity Photon Setup (DHIPS) [29] at the Darmstadt Superconducting Electron Linear Accelerator (S-DALINAC). Bremsstrahlung photons are generated by stopping a monoenergetic electron beam in a thick copper radiator. The bremsstrahlung beam passes a copper collimator before radiating the scattering target which is surrounded by three high-purity Germanium detectors (two at 127° and one at 90° with respect to the incident beam). The latter are surrounded with active Compton suppression shields made of bismuth germanate. The entire setup is shielded by lead against background radiation. The absorber target was placed at the end of the collimator system such that radiation scattered in the absorber was shielded from the detectors. For a more detailed description of the setup, see Ref. [29].

The self-absorption experiment was composed of three individual measurements each at a bremsstrahlung end-point energy of 8.0 MeV. One with (98 h) and one without (97 h) the absorption target in front of the scatterer and the normalization target and an additional measurement (70 h) with absorber target but no scatterer in order to test whether the detectors are properly shielded against radiation from the absorber target.

The scatterer consisted of 2.4 g CeO_2 enriched to 99.5% in ^{140}Ce, the absorber of 59.3 g naturally composed CeO_2, and the normalization target of 312 mg ^{11}B enriched to 99.5%.

4. Analysis

Fig. 1 shows measured spectra in the energy range between 6 MeV and 7 MeV. Although the measuring times were nearly the same and beam conditions were not changed, the measured intensity with absorber is significantly smaller as without absorber due to absorption effects. Despite the shielding of the detectors against the absorber, a small part of the photons stemming from the absorption target are detected. Thus, the spectrum recorded with absorber was not only corrected for atomic attenuation using the factor f as explained above, but also for contributions from the absorber which, however, are small. For both corrections, the spectra are normalized using the well known transitions in ^{11}B. The lower spectrum (green) represents the difference of the measured spectra with and without absorption target after the corrections. Hence, the negative peaks visualize the resonant absorption.

In the analysis of the spectrum measured without absorber ('standard' NRF measurement) we found results for Γ_0^2/Γ that are in average 40% smaller than results of an NRF measurement published in Ref. [10]. However, they agree well with a second, unpublished measurement on ^{140}Ce that we performed independently. Consequently, in the following we rely on our results for Γ_0^2/Γ.

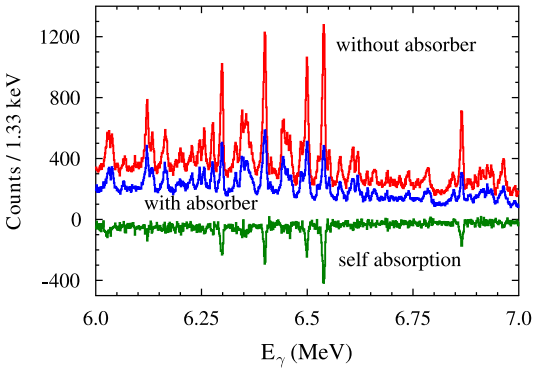

Fig. 1. (Color online.) Spectra recorded during the self-absorption experiment. The upper one (red) corresponds to the measurement without absorber, the middle one (blue) was recorded with the absorption target. The lower spectrum (green) corresponds to the difference of the spectra recorded with (after correction for atomic attenuation effects) and without absorber.

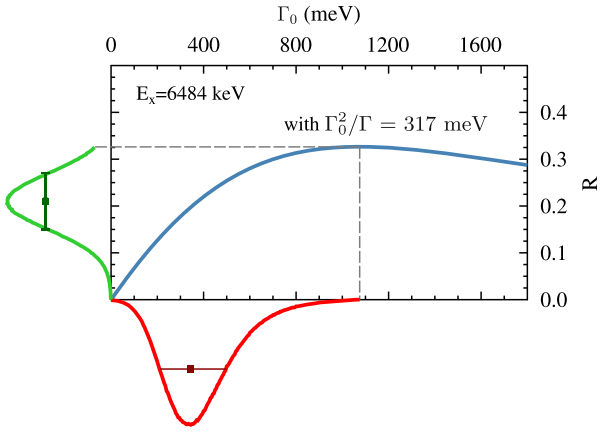

Fig. 2. (Color online.) Self absorption $R_{\Gamma_0,\Gamma}$ of the level at 6484 keV excitation energy in ^{140}Ce. The blue curve was calculated with the condition $\Gamma_0^2/\Gamma = 317$ meV. The experimental result for R is represented via the green square and the according Gaussian distribution. The distribution for Γ_0 (red) is obtained by projecting the distribution of R (green) to the Γ_0 axis.

For the determination of Γ_0 and, hence, Γ_0/Γ the self absorption R_{exp} was evaluated individually for each detector according to Eq. (2). Finally, for each observed state the weighted average of R_{exp} was compared to the computed self absorption $R_{\Gamma_0,\Gamma}$ [Eq. (7)] with Γ_0^2/Γ fixed to the value extracted from the NRF measurement. Fig. 2 shows $R_{\Gamma_0,\Gamma}$ as a function of Γ_0 using the example of the 6484 keV level of ^{140}Ce with $\Gamma_0^2/\Gamma = 317$ meV. The green square and distribution represent the experimentally deduced value $R_{\text{exp}} = 0.21(6)$. The calculated curve (shown in blue) exhibits a maximum since the ratio Γ_0^2/Γ is fixed by the NRF measurement. Thus, when Γ_0 increases, Γ has to increase quadratically which reduces the value of $\sigma(E)$. This leads to a less distinct absorption line and a smaller $R_{\Gamma_0,\Gamma}$. Therefore, in principle, two results for Γ_0 can be determined for one experimental value R_{exp}. However, we will exclusively present the first solution at smaller Γ_0 in the following since the second one normally corresponds to unlikely large values for Γ. In the given example the first solution yields $\Gamma_0 = 0.34^{+0.16}_{-0.13}$ eV and $\Gamma = 0.24^{+0.42}_{-0.18}$ eV, whereas the second solution would be given by $\Gamma_0 = 2.6^{+1.2}_{-0.8}$ eV and $\Gamma = 16.4^{+24.7}_{-9.9}$ eV.

The results for Γ_0 and Γ_0/Γ were determined with help of a Bayesian data analysis [30,31] which basically differs in two points from a conventional analysis. First of all, in the Bayesian approach probability density functions (PDFs) are used to describe measured and resulting quantities instead of discrete numbers as the

conventional (frequentist) approach does. Secondly, it exploits the principle of maximum information entropy [32,33]. This principle foresees to take additional information on the measured and resulting quantities, *i.e.*, constraining conditions, into account.

Radiation measurements are a prominent application area of this analyzing technique. For instance, the activity $A \pm dA$ of a radioactive source can be described with a Gaussian distribution around A with the width given by dA. In the case that A is close to zero or dA is rather large, the distribution may reach into the region below zero. However, an activity cannot be negative. Thus, according to the principle of maximum information entropy, the Gaussian distribution is folded with a step function being zero below zero and one above zero such that this additional information is taken into account and the negative, non-physical part of the distribution is excluded.

In the present case, the uncertainty of the experimentally determined value R_{exp} is Gaussian distributed and, consequently, a Gaussian distribution was chosen as PDF for R_{exp} (see Fig. 2, green curve). Obviously, negative values of R are not physical (they correspond to negative values of Γ_0). Also, values of R_{exp} larger than the maximum R_{max} in the self-absorption curve $R_{\Gamma_0,\Gamma}$ (blue) cannot be treated. Therefore, applying Bayes' theorem, the PDF of R_{exp} is folded with a rectangular function which excludes physically forbidden regions:

$$g(R_{\mathrm{exp}}) = \begin{cases} 1 & \text{for } \ 0 \le R_{\mathrm{exp}} \le R_{\mathrm{max}} \\ 0 & \text{else} \end{cases} . \tag{8}$$

For the resulting distribution of R_{exp}, a corresponding distribution for the ground-state transition width $\Gamma_0(R_{\mathrm{exp}})$ is determined using $R_{\Gamma_0,\Gamma}$ (see Fig. 2, red curve).

In a similar way, the probability distribution of Γ_0/Γ is determined. Starting from the probability distributions of Γ_0 and Γ_0^2/Γ (which is Gaussian) randomly chosen values of Γ_0 and Γ_0^2/Γ are picked to calculate Γ_0/Γ. Repeating this procedure 10^6 times yields the distribution of Γ_0/Γ. Eventually, this distribution for Γ_0/Γ is folded with a step function such that $0 \le \Gamma_0/\Gamma \le 1$ holds. Non-physical values for the branching ratio to the ground state are excluded in this way. In the following, the most probable value defined by the maximum of the PDF and the smallest interval containing 68.3% of the PDF are presented analogous to the 1σ region of a Gaussian distribution.

5. Results and discussion

In total, the self absorption was determined for 104 dipole excited states of ^{140}Ce in the energy range between 3.5 MeV and 7.5 MeV. The corresponding results for the ground-state transition widths $\Gamma_0^{\mathrm{SA}} = \Gamma_0(R_{\mathrm{exp}})$ obtained from self absorption (SA) are shown in Fig. 3 a) as a function of $(\Gamma_0^2/\Gamma)^{\mathrm{NRF}}$ measured in NRF. For better clarity, a double-logarithmic scale with an offset of +1 meV for Γ_0 was chosen. Large uncertainties of R_{exp}, especially for weakly excited states which lead to low statistics, are reflected in large confidence intervals of Γ_0^{SA}. The corresponding results are often located in the physically forbidden region below the green line which marks $\Gamma_0^{\mathrm{SA}} = (\Gamma_0^2/\Gamma)^{\mathrm{NRF}}$, *i.e.*, $\Gamma_0/\Gamma = 1$. This may be attributed to the rather low statistics in these cases. Nevertheless, within the large confidence intervals they also agree with $\Gamma_0/\Gamma = 1$. Only in few cases, Γ_0^{SA} has been found to be significantly smaller than $(\Gamma_0^2/\Gamma)^{\mathrm{NRF}}$ even within the confidence interval. This would correspond to apparently non-physical branching ratios to the ground state. However, those cases may be attributed to single peaks observed in the measured spectra that correspond to two levels being located in such a close proximity that they cannot be resolved within the experimental resolution. As a consequence, the self absorption of the supposedly single state with

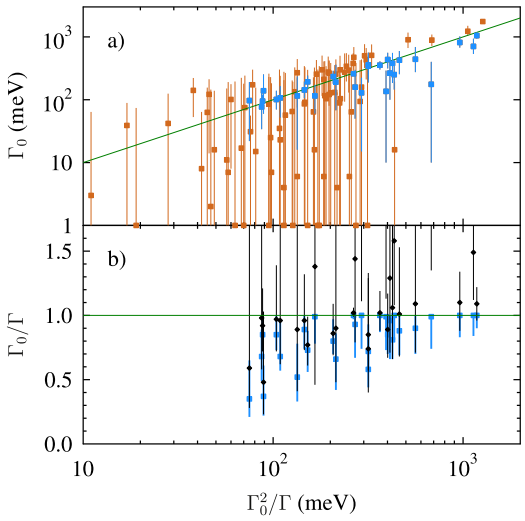

Fig. 3. (Color online.) Most probable values and corresponding confidence intervals for (a) the ground-state transition width Γ_0 and (b) the branching ratio Γ_0/Γ to the ground state determined from the self-absorption measurement exploiting Bayes' theorem. The black diamonds represent the result for Γ_0/Γ as obtained in a direct comparison of R_{exp} with $R_{\Gamma_0,\Gamma}$. The green lines mark physical limits. The branching ratio Γ_0/Γ to the ground state should not exceed 1. Consequently, Γ_0 should not be smaller than Γ_0^2/Γ. See the text for details.

an effective absorption cross section given by the sum of both levels $[(\Gamma_0^2/\Gamma)_{\mathrm{eff}}^{\mathrm{NRF}} = \sum(\Gamma_0^2/\Gamma)_i]$ would be overestimated with respect to the true self-absorption values corresponding to the individual widths $\Gamma_{0,i}^{\mathrm{SA}}$. This results in a too large or even non-physical value of the branching ratio $(\Gamma_0/\Gamma)_{\mathrm{eff}} = (\Gamma_0^2/\Gamma)_{\mathrm{eff}}^{\mathrm{NRF}}/\Gamma_0^{\mathrm{SA}}$ to the ground state of the supposedly single level.

In contrast to Γ_0, large uncertainties of R_{exp} are not properly reflected in Γ_0/Γ since physically forbidden regions are excluded applying Bayes' theorem. Thus, Γ_0/Γ was only determined when R_{exp} was larger than 0 and smaller than R_{max} within its 1σ interval. This condition holds for 29 excited states observed in this work. They are marked in blue in Fig. 3 a) and the corresponding results for Γ_0/Γ are shown with blue squares and the 68.3% confidence interval in Fig. 3 b). For comparison, the black diamonds represent the results for Γ_0/Γ that are obtained in a conventional way by calculating $\Gamma_0(R_{\mathrm{exp}})$ and combining the result with Γ_0^2/Γ from the NRF measurement without applying Bayes' theorem and probability density functions. The given classical uncertainties are maximal errors since they cannot properly be determined from asymmetric uncertainties. An upper limit is introduced for $\Gamma_0/\Gamma \le 1$ with Bayes' theorem and, consequently, the blue squares are systematically shifted to lower values. They are still in agreement with the maximal uncertainties of the conventional approach and are restricted to physical values.

Fig. 3 demonstrates that strongly excited states have ground-state branching ratios of or close to $\Gamma_0/\Gamma = 1$ while the weaker excited states typically exhibit $\Gamma_0/\Gamma < 1$ and, thus, significantly decay also to lower-lying excited levels. To study, whether this trend can be described within the statistical model, the b_0 value expressing the weighted, averaged branching to the ground state was extracted for different regions of Γ_0^2/Γ from both, the experiment as well as a calculation based on the statistical model, respectively. It is defined as

$$b_0 = \frac{\sum_i (\Gamma_0^2/\Gamma)_i}{\sum_i \Gamma_{0,i}}, \tag{9}$$

with i running over all observed levels.

The experimental value $b_{0,\mathrm{exp}}$ was determined analogously to Γ_0/Γ taking all 29 excited states into account for which the

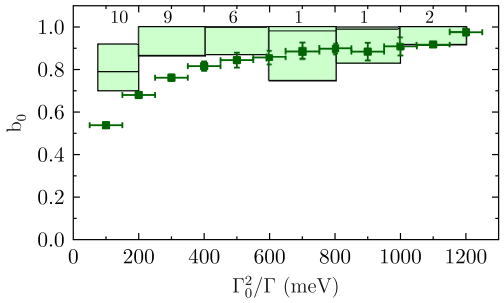

Fig. 4. (Color online.) Results for b_0 from experiment (green boxes) and DICEBOX (green squares) as function of Γ_0^2/Γ. The numbers at the top show how many levels were taken into account to deduce the experimental value.

condition $0 > R_{\mathrm{exp}} > R_{\mathrm{max}}$ holds (see above). For each level i, values for Γ_0^2/Γ and Γ_0 were randomly chosen from the corresponding PDFs and summed up to calculate b_0 according to Eq. (9). This step was repeated 10^6 times for each bin of Γ_0^2/Γ yielding the PDF of $b_{0,\mathrm{exp}}$ for each bin. Eventually, non-physical parts of the PDF have been excluded applying a step function such that $0 \leq b_{0,\mathrm{exp}} \leq 1$.

The calculation was conducted exploiting the DICEBOX code [26] that was adapted for NRF measurements. DICEBOX generates so-called nuclear realizations of level schemes for nuclei according to a given level density parameterization. Furthermore, partial decay widths are passed to each level within such a nuclear realization. These widths are randomly chosen according to photon strength functions provided by the user. Thereby, the effect of Porter–Thomas fluctuations [34] is taken into account, as well. As a next step, γ-ray cascades are simulated within such a nuclear realization. Since different observables such as the excitation energies, spin and parity quantum numbers or the partial decay widths can be extracted for each level that has been part of a γ-ray cascade, the simulation can be analyzed in exactly the same way as a real NRF measurement. Hence, among others, the averaged branching ratio $b_{0,\mathrm{dice}}$ can be determined. A more detailed description of the code and its functionality can be found in Ref. [26].

As input for DICEBOX, the following parameterizations were used. The level density above 3.1 MeV was described in the back-shifted Fermi gas (BSFG) model with parameters determined according to Ref. [35] while for lower energies the known level scheme was included. For the parameterization of the photon-strength functions (PSFs) single Lorentzians were used. The $E1$ parameters stem from a fit to (γ, n) data [36]. Parameters for the $M1$ PSF were determined according to a global parameterization of $M1$ spin-flip resonances as proposed in Ref. [37]. Corresponding values for the $E2$ PSF were determined exploiting a global parameterization introduced in Ref. [38].

With this input, 30 nuclear realizations have been created for each bin of Γ_0^2/Γ and $2 \cdot 10^5$ γ-ray cascades have been simulated within each nuclear realization.

The obtained results for $b_{0,\mathrm{exp}}$ and $b_{0,\mathrm{dice}}$ are shown in Fig. 4 as function of Γ_0^2/Γ. The boxes represent the confidence intervals of $b_{0,\mathrm{exp}}$; the lines within the boxes show the most probable experimental values. The results $b_{0,\mathrm{dice}}$ from DICEBOX are given by small squares. The widths represent the bin sizes for Γ_0^2/Γ. In addition, the numbers of levels per bin available to determine $b_{0,\mathrm{exp}}$ are given at the top of the figure.

In contrast to some individual branching ratios to the ground state (see Fig. 3), $b_{0,\mathrm{exp}}$ does not or only weakly decreases towards weaker excited states. This trend is reproduced by the statistical model. However, the absolute b_0 values extracted from the DICEBOX calculation agree with the experimental results $b_{0,\mathrm{exp}}$ only for states with elastic NRF widths $\Gamma_0^2/\Gamma \gtrsim 600$ meV. For smaller values one observes larger average ground-state branching ratios b_0 than estimated from the statistical model calculation.

Interestingly, the previous literature [20,22,23] reported that b_0 as a function of excitation energy was difficult to be described within the statistical model. A maximum of b_0 in the energy domain of the PDR has, *e.g.*, been reported for ^{94}Mo [23] and for ^{130}Te [22], whereas b_0 calculated within the statistical model steadily decreases as a function of increasing energy. This deviation may occur because the statistical model can either not describe the decay behavior of the strongly excited states that are concentrated in the excitation-energy domain of the PDR where also the maximum of b_0 is observed or because the statistical model cannot describe the concentration of strongly excited states in this excitation-energy range. However, the results from Refs. [22, 23] cannot decide on this alternative since not individual states but groups of excited states with various excitation strengths in excitation-energy bins have been investigated in Refs. [22,23].

In contrast to that, we analyzed here individual states and, consequently, it became possible to probe the reliability of the statistical model also as a function of the excitation strength in terms of Γ_0^2/Γ. In the light of our findings we must conclude that the local enhancement of b_0 in Refs. [22,23] must not only originate from a non-statistical concentration of strongly excited states, but originates at least partly also from an underestimation of the decay branching ratio of more weakly excited states by the statistical model. This emphasizes the conclusion of a non-statistical structure in the energy domain of the PDR made in Ref. [23]. Unfortunately, both observations stem from data on different nuclei potentially inducing a systematical error on our conclusion. Further systematical studies are desirable to clarify the situation.

6. Conclusion

In this work, a pioneering self-absorption experiment was applied to determine the ground-state transition width Γ_0 of states contributing to the PDR directly in a model-independent way. Even at rather high level densities, like in the PDR region, we were able to extract Γ_0 for individual states. Due to the improved normalization technique with respect to earlier measurements it was possible to determine Γ_0 also for weaker excited states. With thicker absorption targets that are better suited to address weakly excited states, the uncertainties for those levels can further be improved.

A comparison of the experimental average branching ratio $b_{0,\mathrm{exp}}$ to the ground state with results from statistical model calculations revealed that b_0 is larger than estimated by the statistical model for $\Gamma_0^2/\Gamma \lesssim 600$ meV. This observation supports the interpretation of the PDR as a non-statistical structure from the previous literature. With this work, we demonstrated that self absorption is a powerful method to study Γ_0 of individual states and to provide valuable insight into the decay pattern of low-lying dipole states.

Acknowledgements

The authors would like to thank the S-DALINAC operating team for providing excellent beam conditions. Furthermore, we cordially acknowledge the help of all scientists on shift during the measurements. We also thank M. Krtička for providing the DICEBOX code. A.E. acknowledges support by HIC for FAIR.

This work was supported by the Deutsche Forschungsgemeinschaft (Contract No. SFB 634 and SO907/2-1) and by the Alliance Program of the Helmholtz Association (HA216/EMMI).

References

[1] D. Savran, T. Aumann, A. Zilges, Prog. Part. Nucl. Phys. 70 (2013) 210–245.

[2] S. Goriely, Phys. Lett. B 436 (1998) 10–18.
[3] S. Goriely, E. Khan, M. Samyn, Nucl. Phys. A 739 (2004) 331–352.
[4] E. Litvinova, H. Loens, K. Langanke, G. Martínez-Pinedo, T. Rauscher, P. Ring, F.-K. Thielemann, V. Tselyaev, Nucl. Phys. A 823 (2009) 26–37.
[5] B. Alex Brown, Phys. Rev. Lett. 85 (2000) 5296–5299.
[6] R. Furnstahl, Nucl. Phys. A 706 (2002) 85–110.
[7] N. Paar, D. Vretenar, E. Khan, G. Colò, Rep. Prog. Phys. 70 (2007) 691.
[8] J. Endres, E. Litvinova, D. Savran, P.A. Butler, M.N. Harakeh, S. Harissopulos, R.-D. Herzberg, R. Krücken, A. Lagoyannis, N. Pietralla, V.Yu. Ponomarev, L. Popescu, P. Ring, M. Scheck, K. Sonnabend, V.I. Stoica, H.J. Wörtche, A. Zilges, Phys. Rev. Lett. 105 (2010) 212503.
[9] R. Schwengner, R. Massarczyk, G. Rusev, N. Tsoneva, D. Bemmerer, R. Beyer, R. Hannaske, A.R. Junghans, J.H. Kelley, E. Kwan, H. Lenske, M. Marta, R. Raut, K.D. Schilling, A. Tonchev, W. Tornow, A. Wagner, Phys. Rev. C 87 (2013) 024306.
[10] S. Volz, N. Tsoneva, M. Babilon, M. Elvers, J. Hasper, R.-D. Herzberg, H. Lenske, K. Lindenberg, D. Savran, A. Zilges, Nucl. Phys. A 779 (2006) 1.
[11] G. Rusev, R. Schwengner, R. Beyer, M. Erhard, E. Grosse, A.R. Junghans, K. Kosev, C. Nair, K.D. Schilling, A. Wagner, F. Dönau, S. Frauendorf, Phys. Rev. C 79 (2009) 061302(R).
[12] M. Scheck, V.Yu. Ponomarev, M. Fritzsche, J. Joubert, T. Aumann, J. Beller, J. Isaak, J.H. Kelley, E. Kwan, N. Pietralla, R. Raut, C. Romig, G. Rusev, D. Savran, L. Schorrenberger, K. Sonnabend, A.P. Tonchev, W. Tornow, H.R. Weller, A. Zilges, M. Zweidinger, Phys. Rev. C 88 (2013) 044304.
[13] F.R. Metzger, Prog. Nucl. Phys. 7 (1959) 53.
[14] U. Kneissl, H. Pitz, A. Zilges, Prog. Part. Nucl. Phys. 37 (1996) 349–433.
[15] R. Schwengner, G. Rusev, N. Tsoneva, N. Benouaret, R. Beyer, M. Erhard, E. Grosse, A.R. Junghans, J. Klug, K. Kosev, H. Lenske, C. Nair, K.D. Schilling, A. Wagner, Phys. Rev. C 78 (2008) 064314.
[16] R. Massarczyk, R. Schwengner, F. Dönau, E. Litvinova, G. Rusev, R. Beyer, R. Hannaske, A.R. Junghans, M. Kempe, J.H. Kelley, T. Kögler, K. Kosev, E. Kwan, M. Marta, A. Matic, C. Nair, R. Raut, K.D. Schilling, G. Schramm, D. Stach, A.P. Tonchev, W. Tornow, E. Trompler, A. Wagner, D. Yakorev, Phys. Rev. C 86 (2012) 014319.
[17] N. Pietralla, Z. Berant, V.N. Litvinenko, S. Hartman, F.F. Mikhailov, I.V. Pinayev, G. Swift, M.W. Ahmed, J.H. Kelley, S.O. Nelson, R. Prior, K. Sabourov, A.P. Tonchev, H.R. Weller, Phys. Rev. Lett. 88 (2001) 012502.
[18] H.R. Weller, M.W. Ahmed, H. Gao, W. Tornow, Y.K. Wu, M. Gai, R. Miskimen, Prog. Part. Nucl. Phys. 62 (2009) 257–303.
[19] A.P. Tonchev, S.L. Hammond, J.H. Kelley, E. Kwan, H. Lenske, G. Rusev, W. Tornow, N. Tsoneva, Phys. Rev. Lett. 104 (2010) 072501.
[20] C.T. Angell, S.L. Hammond, H.J. Karwowski, J.H. Kelley, M. Krtička, E. Kwan, A. Makinaga, G. Rusev, Phys. Rev. C 86 (2012) 051302.
[21] M. Scheck, V.Yu. Ponomarev, T. Aumann, J. Beller, M. Fritzsche, J. Isaak, J.H. Kelley, E. Kwan, N. Pietralla, R. Raut, C. Romig, G. Rusev, D. Savran, K. Sonnabend, A.P. Tonchev, W. Tornow, H.R. Weller, M. Zweidinger, Phys. Rev. C 87 (2013) 051304.
[22] J. Isaak, D. Savran, M. Krtička, M. Ahmed, J. Beller, E. Fiori, J. Glorius, J. Kelley, B. Löher, N. Pietralla, C. Romig, G. Rusev, M. Scheck, L. Schnorrenberger, J. Silva, K. Sonnabend, A. Tonchev, W. Tornow, H. Weller, M. Zweidinger, Phys. Lett. B 727 (2013) 361–365.
[23] C. Romig, J. Beller, J. Glorius, J. Isaak, J.H. Kelley, E. Kwan, N. Pietralla, V.Y. Ponomarev, A. Sauerwein, D. Savran, M. Scheck, L. Schnorrenberger, K. Sonnabend, A.P. Tonchev, W. Tornow, H.R. Weller, A. Zilges, M. Zweidinger, Phys. Rev. C 88 (2013) 044331.
[24] A. Tamii, I. Poltoratska, P. von Neumann-Cosel, Y. Fujita, T. Adachi, C.A. Bertulani, J. Carter, M. Dozono, H. Fujita, K. Fujita, K. Hatanaka, D. Ishikawa, M. Itoh, T. Kawabata, Y. Kalmykov, A.M. Krumbholz, E. Litvinova, H. Matsubara, K. Nakanishi, R. Neveling, H. Okamura, H.J. Ong, B. Özel-Tashenov, V.Yu. Ponomarev, A. Richter, B. Rubio, H. Sakaguchi, Y. Sakemi, Y. Sasamoto, Y. Shimbara, Y. Shimizu, F.D. Smit, T. Suzuki, Y. Tameshige, J. Wambach, R. Yamada, M. Yosoi, J. Zenihiro, Phys. Rev. Lett. 107 (2011) 062502.
[25] N. Pietralla, I. Bauske, O. Beck, P. von Brentano, W. Geiger, R.-D. Herzberg, U. Kneissl, J. Margraf, H. Maser, H.H. Pitz, A. Zilges, Phys. Rev. C 51 (1995) 1021–1024.
[26] F. Bečvář, Nucl. Instrum. Methods Phys. Res. A 417 (1998) 434.
[27] V.K. Rasmussen, C.P. Swann, Phys. Rev. 183 (1969) 918–923.
[28] R. Vodhanel, M.K. Brussel, R. Moreh, W.C. Sellyey, T.E. Chapuran, Phys. Rev. C 29 (1984) 409–417.
[29] K. Sonnabend, D. Savran, J. Beller, M. Büssing, A. Constantinescu, M. Elvers, J. Endres, M. Fritzsche, J. Glorius, J. Hasper, J. Isaak, B. Löher, S. Müller, N. Pietralla, C. Romig, A. Sauerwein, L. Schnorrenberger, C. Wälzlein, A. Zilges, M. Zweidinger, Nucl. Instrum. Methods Phys. Res. A 640 (2011) 6–12.
[30] K. Weise, W. Wöger, Meßunsicherheit und Meßdatenauswertung, Wiley–VCH, 1999.
[31] K. Weise, K. Hübel, E. Rose, M. Schläger, D. Schrammel, M. Täschner, R. Michel, Radiat. Prot. Dosim. 121 (2006) 52–63.
[32] E.T. Jaynes, Phys. Rev. 106 (1957) 620–630.
[33] E.T. Jaynes, R.D. Rosenkrantz (Eds.), Papers on Probability, Statistics and Statistical Physics, Kluwer Academic Publishers, Dordrecht, The Netherlands, 1989.
[34] C.E. Porter, R.G. Thomas, Phys. Rev. 104 (1956) 483–491.
[35] T.v. Egidy, D. Bucurescu, Phys. Rev. C 72 (2005) 044311.
[36] A. Leprêtre, H. Beil, R. Bergère, P. Carlos, J. Fagot, A.D. Miniac, A. Veyssière, H. Miyase, Nucl. Phys. A 258 (1976) 350–364.
[37] T. Belgya, O. Bersillon, R. Capote, T. Fukahori, G. Zhigang, S. Goriely, M. Herman, A. Ignatyuk, S. Kailas, A. Koning, P. Oblozinsky, V. Plujko, P. Young, Handbook for Calculations of Nuclear Reaction Data, RIPL-2, IAEA-TECDOC-1506, IAEA, Vienna, 2006.
[38] W. Prestwich, M. Islam, T. Kennett, Z. Phys. A 315 (1984) 103–111.